J. Biochem. 2009;146(4)509–521
doi:10.1093/jb/mvp094

Insights into the Enzyme–Substrate Interaction in the Norovirus 3C-like Protease

Yuichi Someya* and Naokazu Takeda

Department of Virology II, National Institute of Infectious Diseases, 4-7-1 Gakuen, Musashi-Murayama, Tokyo 208-0011, Japan

Received May 8, 2009; accepted June 11, 2009; published online June 24, 2009

The Glu54 residue of the norovirus 3C-like protease was implicated in proteolysis as a third-member carboxylate of the catalytic triad. The E54L mutant protease cleaved the sequence ^{133}LSFE/AP between the 3B and 3C regions of norovirus polyprotein, but did not cleave the sequence ^{198}ATSE/GK between the 3A and 3B. The 3BC junction mutation (3B-L133A or 3B-F135S) hampered the cleavage by the E54L protease, whereas the 3AB junction mutation (3A-A198L, S200F) allowed the E54L protease to digest. These results indicate that the E54L mutant protease is a substrate-specificity mutant and requires large hydrophobic amino acid residues at both P4 and P2 positions of the substrate. It was notable that the 3A-S200F P2 position mutation caused tight interaction between the wild-type protease and the C-terminus of the 3A protein, hence a decreased release rate of the product from the enzyme. This tight binding was dependent on the hydrophobicity of amino acid residues introduced at position 200 of the 3A region and was affected by the mutation in the bII-cII loop of the protease or the mutation of position 198 of 3A corresponding to the P4 position of the substrate. These results suggest that the protease and the substrate sense each other in the process of the proteolysis, being supported by crystal structures.

Key words: norovirus, 3C-like protease, catalytic triad, serine-like cysteine protease, substrate specificity.

Abbreviations: GST, glutathione S-transferase; NTPase, nucleotide tripphosphatase; ORF, open-reading frame; VPg, genome-linked viral protein.

Norovirus is a major cause of acute non-bacterial gastroenteritis in humans, and genetically and antigenically diverse strains have been isolated worldwide (*1*–*3*). Norovirus, a member of the family *Caliciviridae*, is a positive-sense single-stranded RNA virus. The norovirus genome is ~7.7 kb in length with a poly(A) tail at its 3′-end. VPg, a genome-linked viral protein, is believed to be bound to the 5′-end in place of the cap structure (*4*).

The genome encodes three open-reading frames (ORFs) (*5*). The ORF1 product is a polyprotein and is cleaved by its viral 3C-like protease activity into six non-structural proteins, which include 2C-like NTPase, 3B VPg and 3D RNA-dependent RNA polymerase, in addition to 3C-like protease (*6*, *7*). The nomenclature is based on that for picornaviruses. The ORF2 and ORF3 products are a major and a minor structural protein (VP1 and VP2), respectively. The norovirus virion consists of 180 VP1 molecules with the VPg-linked RNA genome and VP2 molecules inside. The sequence diversity of the P2 domain of VP1 correlates with the wide variety of the antigenicity among noroviruses (*8*–*10*) and potentially provides different patterns of binding to histo-blood group antigens (*11*).

Norovirus 3C-like protease is a central enzyme that is solely responsible for the maturation of norovirus ORF1 polyprotein (*6*, *7*). The 3C-like proteases of various strains isolated from humans share high amino acid identity and have significant similarity with those of other caliciviruses. Norovirus 3C-like protease is a potent target of medication for the treatment of norovirus diarrhea.

Our extensive mutagenesis study for a 3C-like protease of the Chiba strain revealed that His30 and Cys139 were responsible for proteolysis, the former being considered the general base and the latter the nucleophile in the catalytic centre (*12*). This was clearly revealed by the X-ray crystal structure at 2.8 Å resolution, which showed that the norovirus 3C-like protease had a chymotrypsin-like fold (*13*). The crystal structure also suggested that Glu54, as the third-member carboxylate that interacted with His30, was involved in the catalysis just like typical chymotrypsin-like serine proteases (*13*). This suggested that the mechanism of the proteolysis by the norovirus 3C-like protease was identical to that of chymotrypsin; that is, the thiol of Cys139 attacks a carbonyl carbon of the substrate, followed by protonation of the imidazole ring of His30 by the proton released from the thiol of Cys139. A negatively charged carboxylate of Glu54 interacts with and stabilizes the imidazole ring of His30. However, we had concluded that Glu54 was not essential for the activity because the Glu54-to-Ala mutant protease retained protease activity comparable to that of the wild-type enzyme (*12*).

Our recent study on the saturation mutagenesis of the Glu54 residue reinforced that Glu54 was not essential for the proteolytic activity, and that the proteolysis could be

*To whom correspondence should be addressed.
Tel: +81-42-561-0771, Fax: +81-42-561-4729,
E-mail: someya@nih.go.jp

exerted by the two catalytic residues, His30 and Cys139 (*14*). This report also raised new insight into the role of Glu54 on the substrate specificity, since the E54I, E54L, and E54P mutant proteases cleaved the 3B/3C junction, but did not cleave the 3A/3B junction, when the GST fusion proteins including the 3A, 3B and 3C regions of norovirus polyprotein were used for cleavage assay (*14*). In this study, various mutations were introduced at the 3A/3B and 3B/3C junctions in order to know the amino acid requirement for the cleavage by the E54L mutant protease. Moreover, since we found that an amino acid change in the substrate caused the tight enzyme–substrate interaction, we expanded our investigation to include the molecular basis of this interaction.

MATERIALS AND METHODS

Escherichia coli Strains and Expression Plasmids—The JM109 and HST02 strains (Takara Bio, Inc., Tokyo, Japan) were used for plasmid construction. The BL21-CodonPlus(DE3)-RIPL strain (Stratagene, La Jolla, CA, USA) was used for the expression of the recombinant proteins.

The Glu54 mutations were introduced into an expression plasmid, pGEX-2TK-3aBC, encoding a GST fusion protein to part of the ORF1 polyprotein from the norovirus Chiba strain (Fig. 1) (*14*). The 3A/3B and 3B/3C junction mutations were also introduced into pGEX-2TK-3aBC using the mutagenic oligonucleotides listed in Table 1. All mutations were first detected by the appearance or disappearance of restriction sites, and then verified by DNA sequencing.

For preparation of Chiba virus VPg proteins as antigens, pGEX-6P-VPg was constructed as described below. The VPg-encoding gene fragment was amplified by PCR using VPg-5Bam primer (5′-CCGCCGGATCCGAGGGTA AAAACAAAGGAAAGACCAAGAAAGG-3′) and VPg-3X primer (5′-AGAGCCCGGGCTATTATTCAAAACTGAGTT TTTCATTGTAATCCA-3′) with pUCCVORF1 (*15*) as a template. The *Bam*HI–*Sma*I restriction fragment was transferred to the corresponding position of pGEX-6P-2 (GE Healthcare, Piscataway, NJ, USA).

Preparation of Antisera against Chiba Virus Proteins—Chiba virus 3C-like protease with the N-terminal polyhistidine tag was expressed in *E. coli* BL21-CodonPlus(DE3)-RIPL cells harbouring pUCHisPro (*15*) and purified by passing through TALON Metal Affinity Resin (Clontech, Palo Alto, CA, USA) as described before (*15*). Mice were immunized with purified His-tagged protease, and mouse anti-protease anti-serum was obtained.

Chiba virus VPg proteins were expressed in *E. coli* BL21-CodonPlus(DE3)-RIPL cells harbouring pGEX-6P-VPg, and GST-fused VPg proteins were purified using the ÄKTAprime chromatography system, which is equipped with a GSTrap FF column (GE Healthcare). After digestion of purified GST-fused VPg proteins with PreScission Protease (GE Healthcare), VPg proteins were isolated by trapping the GST moiety with the GSTrap FF column, and were provided by a custom antisera service (Scrum Inc., Tokyo, Japan).

Expression of the Recombinant Proteins in E. coli Cells and SDS–PAGE Analysis of Proteins—*Escherichia coli* BL21-CodonPlus(DE3)-RIPL cells harbouring each of the pGEX-2TK-3aBC plasmids were grown on 4 ml of MagicMedia *E. coli* Expression Medium (Invitrogen, Carlsbad, CA, USA) at 37°C for 24 h, harvested, and resuspended in 600 µl of PBS containing 1.0% Triton X-100. A one-half volume of glass beads (0.1 mm diameter) was added to the cell suspension, followed by vigorous vortexing for 3 min. After centrifugation at 15,000 *g* for 10 min, the supernatant was transferred to a new tube. Proteins were determined with a BCA Protein Assay Kit (Pierce Biotechnology, Rockford, IL, USA) using BSA as a standard.

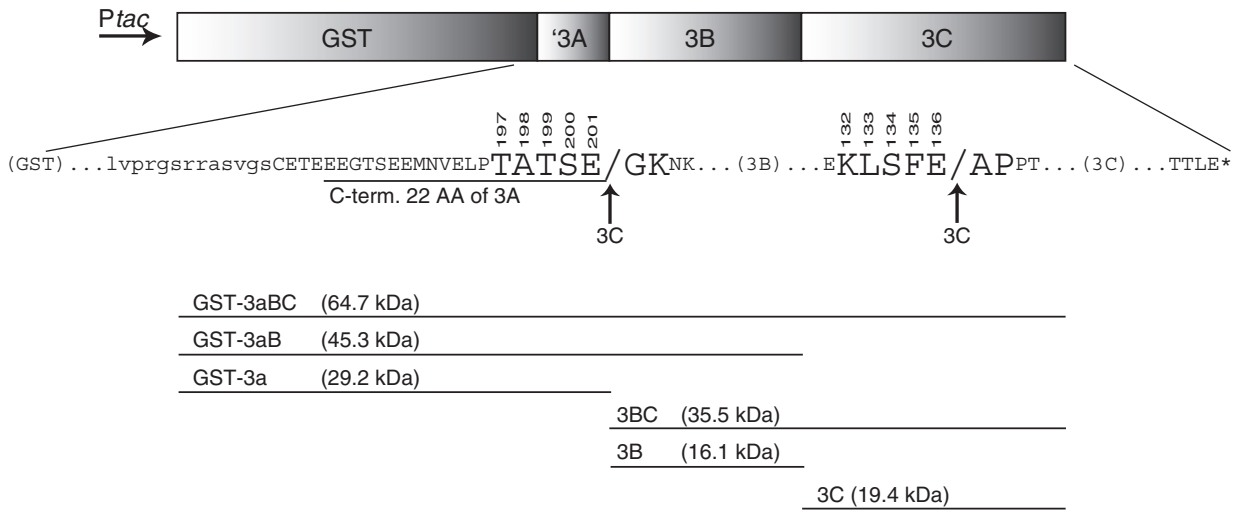

Fig. 1. **Construction of an expression plasmid, pGEX-2TK-3aBC.** The gene fragments encoding the C-terminal 22 amino acid residues of 3A and the entire 3B VPg and 3C-like protease were fused in-frame to the GST gene of the pGEX-2TK vector. The fusion protein, GST-3aBC, has two 3C-like protease recognition sites (TATSE/GK and KLSFE/AP). The calculated molecular weight of the parental protein and possible intermediates along with the final products are shown.

Table 1. **Oligonucleotides used for site-directed mutagenesis.**

Primer	Sequence[a]	Related codon changes	Restriction site
ABtoBC-PSF	5′-CCCACCctcAgTTtTGAGGcgccAAACAAAGGAAAGACCAAGAAA-3′	GCC ACT TCT GAG GGT AAA to CTC AGT TTT GAG GCG CCA	EheI
ABtoBC-PSR	5′-TTTGTTTggcgCCTCAaAAcTgagGGTGGGAAGCTCCACATTCAT-3′		
BCtoAB-PSF	5′-GAAAAAgcCAcTTcTGAgGgtaaACCAACCCTCTGGAGTCGAGTC-3′	CTC AGT TTT GAA GCC CCA to GCC ACT TCT GAG GGT AAA	(XcmI)[b]
BCtoAB-PSR	5′-GGTTGGTttagCgTCAgAAgTGgcTTTTTCATTGTAATCCACTTC-3′		
ATStoLSF-PSF	5′-CCACCttaagTTtTGAGGGTAAAAACAAAGGAAAG-3′	GCC ACT TCT to TTA AGT TTT	BspTI
ATStoLSF-PSR	5′-CCTCAaAActtaaGGTGGGAAGCTCCACATTCATC-3′		
LSFtoATS-PSF	5′-AAAAAgcCAcTagTGAAGCCCCACCAACCCTCTGG-3′	CTC AGT TTT to GCC ACT AGT	SpeI
LSFtoATS-PSR	5′-CTTCActAgTGgcTTTTTCATTGTAATCCACTTCC-3′		
GKtoAP-PSF	5′-TCTGAGGcgccAAACAAAGGAAAGACCAAGAAAGG-3′	GGT AAA to GCG CCA	EheI
GKtoAP-PSR	5′-TTTGTTTggcgCCTCAGAAGTGGCGGTGGGAAGCT-3′		
APtoGK-PSF	5′-TTTTGAAGgCaaACCAACCCTCTGGAGTCGAGTCG-3′	GCC CCA to GGC AAA	(XcmI)[b]
APtoGK-PSR	5′-GGGTTGGTttGcCTTCAAAACTGAGTTTTTCATTG-3′		
3A-A198L-PSF	5′-TTCCCACgttaACTTCTGAGGGTAAAAACAAAGGA-3′	GCC to TTA	HpaI
3A-A198L-PSR	5′-CAGAAGTtaacGTGGGAAGCTCCACATTCATCTCC-3′		
3A-T199S-PSF	5′-CCACCGCtAgcTCTGAGGGTAAAAACAAAGGAAAG-3′	ACT to AGC	NheI
3A-T199S-PSR	5′-CCTCAGAgcTaGCGGTGGGAAGCTCCACATTCATC-3′		
3A-S200F-PSF	5′-GCCACTTtcGAaGGTAAAAACAAAGGAAAGACCAA-3′	TCT to TTC	Bsp119I
3A-S200F-PSR	5′-TTTTACCtTCgaAAGTGGCGGTGGGAAGCTCCACA-3′		
3A-A198L,S200F-PSF	5′-CCACCttaACgTtTGAGGGTAAAAACAAAGGAAAG-3′	GCC & TCT to TTA & TTT	Psp1406I
3A-A198L,S200F-PSR	5′-CCTCAaAcGTtaaGGTGGGAAGCTCCACATTCATC-3′		
3B-L133A-PSF	5′-GAAAAAgcTAGcTTTGAAGCCCCACCAACCCTCTG-3′	CTC to GCT	NheI
3B-L133A-PSR	5′-TTCAAAgCTAgcTTTTTCATTGTAATCCACTTCCC-3′		
3B-S134T-PSF	5′-TGAAAAgtTaAcTTTTGAAGCCCCACCAACCCTCT-3′	AGT to ACT	HpaI
3B-S134T-PSR	5′-TCAAAAgTtAacTTTTCATTGTAATCCACTTCCCT-3′		
3B-F135S-PSF	5′-AAAACTgAGcTcTGAAGCCCCACCAACCCTCTGGA-3′	TTT to TCT	SacI
3B-F135S-PSF	5′-GCTTCAgAgCTcAGTTTTTCATTGTAATCCACTTC-3′		
ATStoMHL-PSF	5′-CCACCatgcaTctTGAGGGTAAAAACAAAGGAAAG-3′	GCC ACT TCT to ATG CAT CTT	EcoT22I
ATStoMHL-PSR	5′-CCTCAagAtgcatGGTGGGAAGCTCCACATTCATC-3′		
ATStoFQM-PSF	5′-CTTCCaACgttCcagatgGAGGGTAAAAACAAAGG-3′	GCC ACT TCT to TTC CAG ATG	Psp1406I
ATStoFQM-PSR	5′-CCTCcatctgGaacGTtGGAAGCTCCACATTCATC-3′		
ATStoTTL-PSF	5′-CCACCaCaACgTtgGAGGGTAAAAACAAAGGAAAG-3′	GCC ACT TCT to ACA ACG TTG	Psp1406I
ATStoTTL-PSR	5′-CCTCcaAcGTtGtGGTGGGAAGCTCCACATTCATC-3′		
3A-S200A-PSF	CCGCCACcgCgGAGGGTAAAAACAAAGGAAAGACC	TCT to GCG	SacII
3A-S200A-PSR	TACCCTCcGcgGTGGCGGTGGGAAGCTCCACATTC		
3A-S200H-PSF	CACCGCCACTcaTGAGGGTAAAAACAAAGG	TCT to CAT	BspHI
3A-S200H-PSR	TTACCCTCAtgAGTGGCGGTGGGAAGCTCC		
3A-S200L-PSF	CCGCCACTctcGAGGGTAAAAACAAAGGAAAGACC	TCT to CTC	XhoI
3A-S200L-PSR	TACCCTCgagAGTGGCGGTGGGAAGCTCCACATTC		
3A-S200M-PSF	CCGCCACcatgGAGGGTAAAAACAAAGGAAAGACC	TCT to ATG	NcoI
3A-S200M-PSR	TACCCTCcatgGTGGCGGTGGGAAGCTCCACATTC		
3A-S200W-PSF	CCGCCACgTggGAGGGTAAAAACAAAGGAAAGACC	TCT to TGG	Eco72I
3A-S200W-PSR	TACCCTCccAcGTGGCGGTGGGAAGCTCCACATTC		
3A-S200Y-PSF	CCGCCACaTaTGAGGGTAAAAACAAAGGAAAGACC	TCT to TAT	NdeI
3A-S200Y-PSR	TACCCTCAtAtGTGGCGGTGGGAAGCTCCACATTC		
I109A-PSF	ATGAAGgcCCAaGGAAGGCTAGTGCATGGT	ATC to GCC	EcoT14I
I109A-PSR	CCTTCCtTGGgcCTTCATGGACGCTATAGC		

(continued)

Table 1. **Continued.**

Primer	Sequence[a]	Related codon changes	Restriction site
Q110A-PSF	AGATCgccGGcAGGCTAGTGCATGGTCAA	CAG to GCC	NaeI
Q110A-PSR	GCCTgCCggcGATCTTCATGGACGCTAT		
R112A-PSF	TCCAGGGAgcGCTAGTGCATGGTCAATCTGGGATG	AGG to GCG	Aor51HI
R112A-PSR	GCACTAGCgcTCCCTGGATCTTCATGGACGCTATA		
V114A-PSF	GAAGGCTAGcGCATGGTCAATCTGGGATGC	GTG to GCG	NheI
V114A-PSR	TGACCATGCgCTAGCCTTCCCTGGATCTTC		
3A-A198G-PSF	CTTCCCACCGgtACcTCTGAGGGTAAAAACAAAGG	GCC to GGT	BshTI, KpnI
3A-A198G-PSR	TACCCTCAGAgGTacCGGTGGGAAGCTCCACATTC		
3A-A198S-PSF	CTTCCCACtagtACTTCTGAGGGTAAAAACAAAGG	GCC to AGT	SpeI
3A-A198S-PSR	CCTCAGAAGTactaGTGGGAAGCTCCACATTCATC		
3A-A198V-PSF	CTTCCCACgGtCACcTCTGAGGGTAAAAACAAAGG	GCC to GTC	BstEII
3A-A198V-PSR	CCTCAGAgGTGaCcGTGGGAAGCTCCACATTCATC		
3A-A198G,S200F-PSF	CCGgtACcTtcGAaGGTAAAAACAAAGGAAAGACC	GCC & TCT to GGT & TTC	BshTI, KpnI, Bsp119I
3A-A198G,S200F-PSR	TACCtTCgaAgGTacCGGTGGGAAGCTCCACATTC		
3A-A198S,S200F-PSF	CCACtagtACTTtcGAaGGTAAAAACAAAGGAAAG	GCC & TCT to TTA & TTC	SpeI, Bsp119I
3A-A198S,S200F-PSR	TACCtTCgaAAGTactaGTGGGAAGCTCCACATTC		
3A-A198V,S200F-PSF	CCACgGtCACcTtcGAaGGTAAAAACAAAGGAAAG	GCC & TCT to TTA & TTC	BstEII, Bsp119I
3A-A198V,S200F-PSR	TACCtTCgaAgGTGaCcGTGGGAAGCTCCACATTC		

[a]Underlines indicate the restriction sites. Mismatch nucleotides are indicated by small letters. [b]Mutagenesis eliminates the original XcmI site.

Extracted proteins were separated by SDS–PAGE, followed by staining with Coomassie Brilliant Blue or western blotting with rabbit polyclonal anti-GST antibody (Abcam, Cambridge, MA, USA), rat anti-VPg or mouse anti-protease antisera.

GST-binding Assay—Cell extract containing 1 mg of protein was applied to a Glutathione Sepharose 4B MicroSpin column (GE Healthcare), followed by low-speed centrifugation (735*g*) for 1 min. Glutathione-resin-bound proteins were eluted with 100 µl of 50 mM Tris–HCl (pH 8.0) buffer containing 10 mM reduced glutathione. A portion (5 µl) of the eluates was analysed by SDS–PAGE.

Gel Filtration Chromatography of Eluates from Glutathione Sepharose Column—Eluates (75 µl) obtained in the GST-binding assay were subjected to a Superdex 75 (GE Healthcare) column (0.9 × 30 cm, bed volume of 19 ml) with PBS used as an elution buffer at a flow rate of 0.2 ml/min. Gel-filtrated eluates were fractionated (each fraction of 400 µl) after sample application.

Modeling of Chiba Virus 3C-like Protease Complex with a Peptide Inhibitor—The crystal structure of the complex of the Southampton virus 3C-like protease with an inhibitor (LGG peptide) (PDB ID: 2IPH) has been recently released. Based on this structure, the structure of Chiba virus protease–LGG peptide complex was modelled using the institutional, web-based PDFAMS Full Automatic Modeling System. The structure model was visualized with MolFeat software (FiatLux, Tokyo, Japan).

Image Analysis of SDS–PAGE Gel—The density of Coomassie Brilliant Blue-stained protein bands on SDS–PAGE gels was measured by ImageJ software (http://rsb.info.nih.gov/ij/).

RESULTS

Effect of the Mutation of the 3A/3B and 3B/3C Junctions on Cleavage by the 3C-like Protease—When the Glu54-to-Leu mutation was introduced into the GST-3aBC fusion protein, only the 3B/3C junction was cleaved, but the 3A/3B junction was not (*14*) (see also lane 'E54L' in Figs 2 and 3). This result raised the possibility that the cleaved E54L 3C-like protease lost proteolytic activity, as well as the possibility that the E54L protease was not able to cleave the 3A/3B junction because of the alteration in the substrate specificity. In this study, to examine the second possibility, various mutations were introduced into both the 3A/3B junction and the 3B/3C junction of the GST-3aBC fusion protein including the wild-type, E54Q, or E54L 3C-like protease. Since neither of the junction mutations caused any significant change in the cleavage pattern by the wild-type protease or the E54Q mutant protease (data not shown), the results of the E54L mutant protease are mainly described below.

First, six consecutive amino acid residues from the P4 position to the P2' position of the 3A/3B junction and the 3B/3C junction were replaced with the six residues from the respective opponents, which were the ABtoBC and BCtoAB mutants. In the E54L- BCtoAB mutant, uncleaved GST-3aBC fusion was accumulated with production of a trace amount of GST-3aB (Figs 2 and 3A), indicating that the E54L mutant protease hardly cleaved either the first or second 3A/3B sequence. On the other hand, the E54L-ABtoBC mutant fusion gave the same pattern as the E54L mutant fusion that showed accumulation of GST-3aB intermediate (Figs 2 and 3). Since the rat anti-VPg anti-serum raised against purified VPg proteins in this study was more sensitive

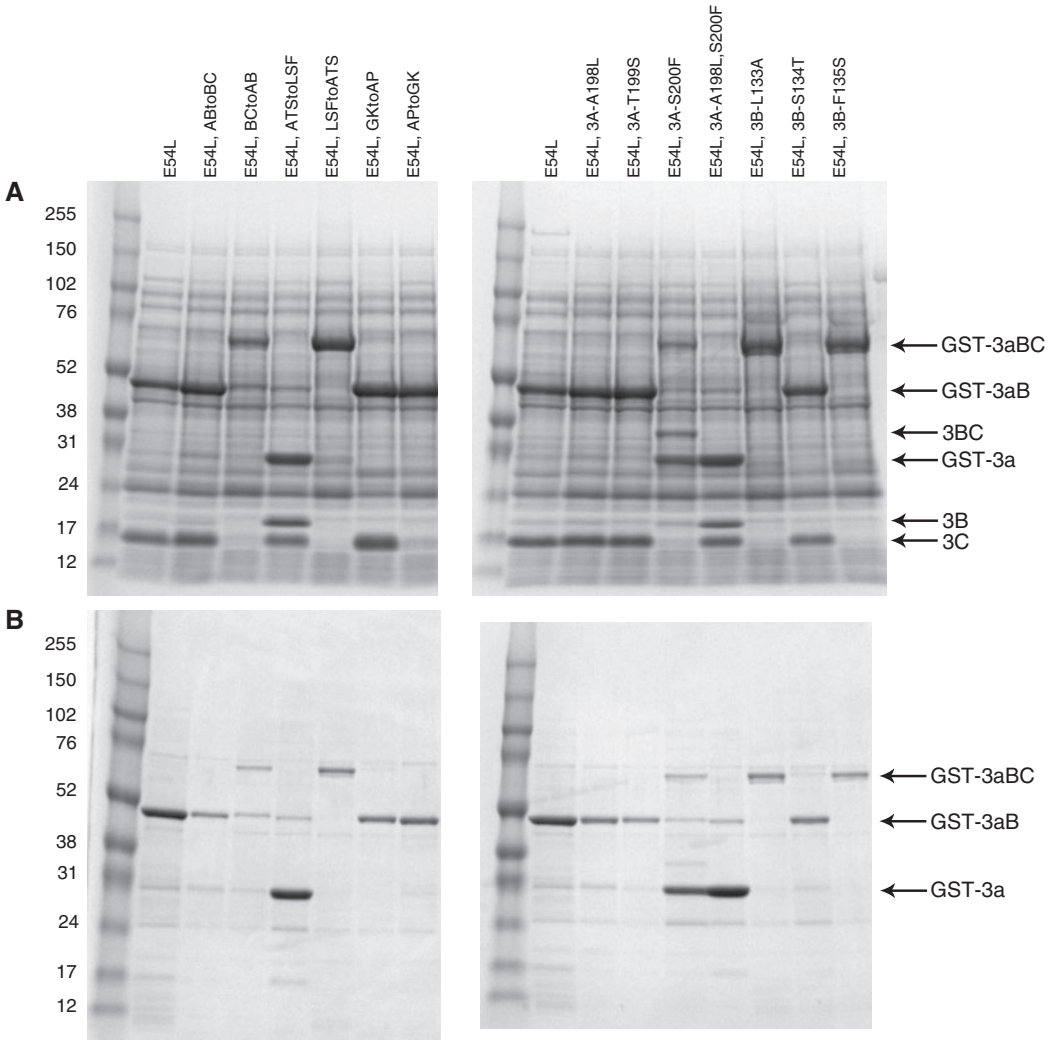

Fig. 2. **Effects of junction mutations on proteolytic cleavage by the E54L 3C-like protease.** (A) Cell extracts (15 μg of proteins) from *E. coli* cells harbouring pGEX-2TK-3aBC plasmid encoding the respective mutations were separated by SDS–PAGE, followed by Coomassie Brilliant Blue staining. The bands corresponding to proteins derived from the expression plasmid are indicated. The respective proteins were confirmed by western blot analysis (Fig. 3 for anti-VPg and anti-Pro, and data not shown for anti-GST). (B) The eluates obtained in the GST-binding assay were subjected to SDS–PAGE, followed by staining. The GST-tagged proteins were also analysed by western blotting with anti-GST (data not shown).

than the rabbit anti-serum prepared before, trace amounts of VPg proteins were detected even in the E54L and E54L-ABtoBC mutants (Fig. 3A). These results clearly suggest that the E54L protease still has proteolytic activity after autolysis of GST-3aBC fusion and has a strict preference for recognition sites. In the ATStoLSF mutant, in which the three amino acid residues from P4 to P2 in the 3A/3B junction were replaced, the two cleavage sites were completely cleaved by the E54L mutant protease, resulting in the production of GST-3a, 3B, and 3C proteins (Figs 2 and 3). On the other hand, the LSFtoATS mutant fusion was not cleaved at all (Figs 2 and 3).

The fusion proteins in which the amino acid residues at the P1' and P2' positions were replaced (GKtoAP and APtoGK) underwent a cleavage event only at the 3B/3C junction, just like the E54L parental mutant fusion (Figs 2 and 3). In the APtoGK fusion, it was apparent that the amount of the cleaved E54L protease was slightly less than the amount of the GST-3aB intermediates (Fig. 2A). This suggested that the protease having the Gly-Lys sequence at its N-terminus might be unstable, although further analysis was not done.

Next, the amino acid residues at the P4, P3, and P2 positions were replaced individually. The P4 (3A-A198L) and P3 (3A-T199S) mutants at the 3A/3B junction gave the same cleavage pattern as the E54L mutant, while the P2 mutant (3A-S200F) gave a different pattern (Figs 2 and 3). That is, the E54L protease produced the GST-3a and 3BC fragments rather than the GST-3aB and 3C fragments, suggesting that the cleavage at the 3A/3B junction including the 3A-S200F mutation preceded the cleavage at the 3B/3C junction. However, the 3A-A198L, S200F double mutant fusion was completely cleaved by

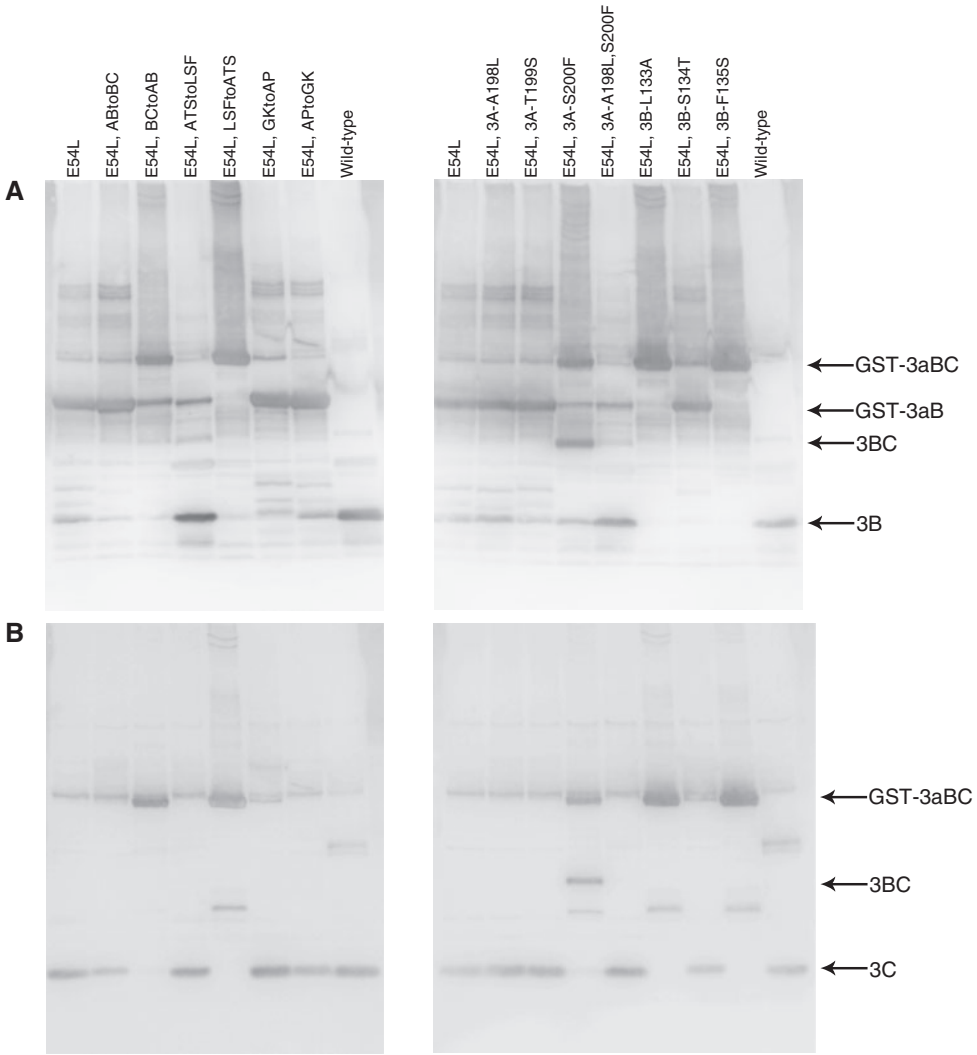

Fig. 3. **Western blot analysis of *E. coli* cell extracts.** Cell extracts (5 μg of proteins) were separated by SDS–PAGE, followed by electroblotting to PVDF membrane. Proteins were detected by rat anti-VPg (A) or mouse anti-protease (B) antibodies. Faint bands that are not indicated with arrows are non-specific, and further analysis was not done.

the E54L mutant protease (Figs 2 and 3). On the other hand, the P4 (3B-L133A) and P2 (3B-F135S) mutations at the 3B/3C junction prevented the E54L protease from cleaving, whereas the P3 (3B-S134T) mutation gave no change in the pattern at all (Figs 2 and 3). As summarized in Table 2, the presence of large hydrophobic amino acid residues at both the P4 and P2 positions like the ATStoLSF and 3A-A198L, S200F mutations allowed the E54L protease to cleave the junction, while the introduction of small amino acid residues at the P4 or P2 positions, such as the LSFtoATS, 3B-L133A and 3B-F135S mutations, completely inhibited the proteolytic cleavage by the E54L protease. These results clearly indicated that the large hydrophobic residues at the P4 and P2 positions were important for cleavage by the E54L mutant protease.

Lastly, the Ala198-Thr199-Ser200 sequence was replaced with the three corresponding amino acid residues from the N-terminal protein/2C, 2C/3A or 3C/3D junction. As shown in Fig. 4, like the ATStoLSF mutant, the ATStoFQM mutant (mimicking the 2C/3A junction) was cleaved by the E54L protease into the GST-3a, 3B and 3C fragments. Similarly, from the ATStoMHL mutant fusion (mimicking the Nt/2C junction), the E54L protease produced three final fragments, although the GST-3aB intermediate also remained. On the other hand, the ATStoTTL mutation (mimicking the 3C/3D junction) hampered the cleavage by the E54L mutant protease. These results also clearly showed the amino acid requirement at the P4 and P2 positions (Fig. 4 and Table 2).

Structure Model of the Peptide Inhibitor Complex of the Chiba Virus 3C-like Protease—As described above, the mutation of the Glu54 residue, which is implicated as the third-member carboxylate in the catalysis, apparently affected the substrate selectivity. In the X-ray structure of the Chiba virus 3C-like protease (*13*), Glu54 is located at the bottom of the S2 hydrophobic pocket that accommodates the P2 side chain of the substrate, and is far away from the P4 position.

Table 2. **Characterization of various mutants.**

Junction mutations	3AB sequence P5-P4-P3-P2-P1-P1'-P2'-P3'	3BC sequence P5-P4-P3-P2-P1-P1'-P2'-P3'	Glu54 mutations		
			None (WT)	E54Q	E54L
None	ThrAlaThrSerGlu/GlyLysAsn	LysLeuSerPheGlu/AlaProPro	+++	+++	GST-3aB + 3C
ABtoBC	Thr**LeuSerPheGlu/AlaPro**Asn	LysLeuSerPheGlu/AlaProPro	+++	+++	GST-3aB + 3C
BCtoAB	ThrAlaThrSerGlu/GlyLysAsn	Lys**AlaThrSerGlu/GlyLys**Pro	+++	+++	–
ATStoLSF	Thr**LeuSerPhe**Glu/GlyLysAsn	LysLeuSerPheGlu/AlaProPro	+++	+++	+++
LSFtoATS	ThrAlaThrSerGlu/GlyLysAsn	Lys**AlaThrSer**Glu/AlaProPro	+++	+++	–
GKtoAP	ThrAlaThrSerGlu/**AlaPro**Asn	LysLeuSerPheGlu/AlaProPro	+++	+++	GST-3aB + 3C
APtoGK	ThrAlaThrSerGlu/GlyLysAsn	LysLeuSerPheGlu/**GlyLys**Pro	+++	+++	GST-3aB + 3C
3A-A198L	Thr**Leu**ThrSerGlu/GlyLysAsn	LysLeuSerPheGlu/AlaProPro	+++	+++	GST-3aB + 3C
3A-T199S	ThrAla**Ser**SerGlu/GlyLysAsn	LysLeuSerPheGlu/AlaProPro	+++	+++	GST-3aB + 3C
3A-S200F	ThrAlaThr**Phe**Glu/GlyLysAsn	LysLeuSerPheGlu/AlaProPro	+++	+++	+
3A-A198L,S200F	Thr**Leu**Thr**Phe**Glu/GlyLysAsn	LysLeuSerPheGlu/AlaProPro	+++	+++	++ ~ +++
3B-L133A	ThrAlaThrSerGlu/GlyLysAsn	Lys**Ala**SerPheGlu/AlaProPro	+++	+++	–
3B-S134T	ThrAlaThrSerGlu/GlyLysAsn	LysLeu**Thr**PheGlu/AlaProPro	+++	+++	GST-3aB + 3C
3B-F135S	ThrAlaThrSerGlu/GlyLysAsn	LysLeuSer**Ser**Glu/AlaProPro	+++	+++	–
ATStoMHL (Nt2C-like)	Thr**MetHisLeu**Glu/GlyLysAsn	LysLeuSerPheGlu/AlaProPro	+++	+++	++
ATStoFQM (2C3A-like)	Thr**PheGlnMet**Glu/GlyLysAsn	LysLeuSerPheGlu/AlaProPro	+++	+++	++ ~ +++
ATStoTTL (3CD-like)	Thr**Thr**Thr**Leu**Glu/GlyLysAsn	LysLeuSerPheGlu/AlaProPro	+++	+++	GST-3aB + 3C

Changed amino acid residues are indicated by bold underlined letters. + + +: GST-3aBC was cleaved into GST-3a, 3B and 3C completely; + +: GST-3a, 3B, and 3C were produced, but part of GST-3aB remained; +: About half of GST-3aBC cleaved into GST-3a and 3BC. Very little of 3B and 3C was observed; –: No cleavage occurred.

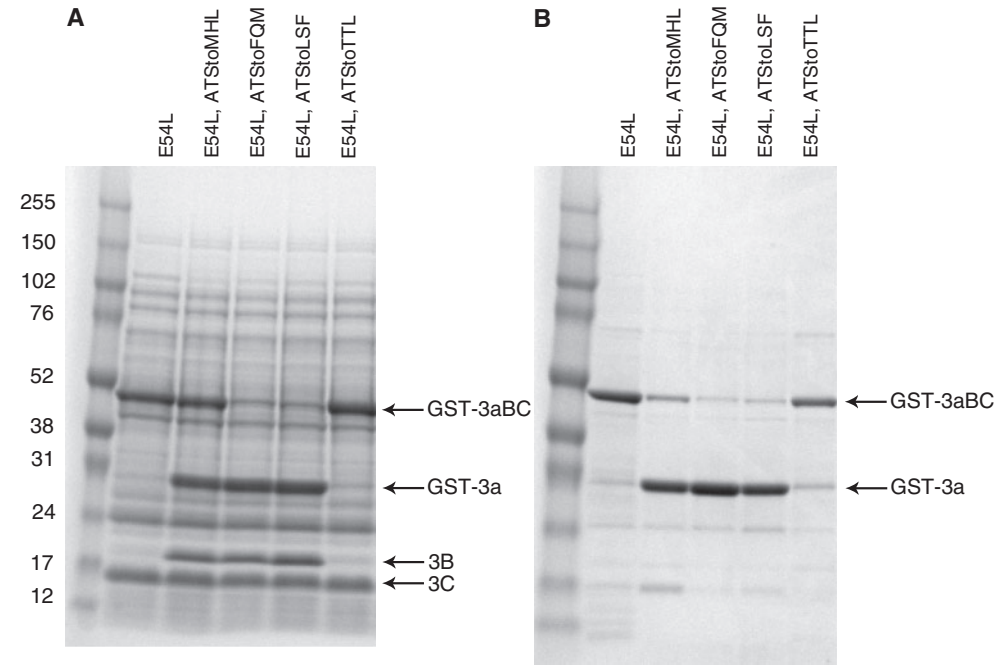

Fig. 4. **Effects of junction mutations on proteolytic cleavage by the E54L 3C-like protease.** Experiments were done in a manner similar to that of Fig. 1. (A) SDS–PAGE of cell extracts including 15 μg of proteins. (B) SDS–PAGE of the eluates obtained in the GST-binding assay.

Recently, the X-ray structure of the 3C-like protease from the Southampton virus (*16*, *17*) has been solved at 1.75 Å resolution as a complex with a peptide inhibitor (LGG peptide) including the P5 to P1 positions (Glu-Phe-Gln-Leu-Gln) corresponding to the cleavage site (PDB ID: 2IPH). These two 3C-like proteases share 90% identity and almost 100% similarity on the amino acid level. Overall structures of these proteases are similar, except that the bII-cII loop (described below) in the inhibitor complex is bent so as to hold the inhibitor. The structure of the Southampton virus protease–inhibitor complex provides a good framework when the molecular aspect of the protease–substrate interaction should be understood. Figure 5 shows the structure model of the

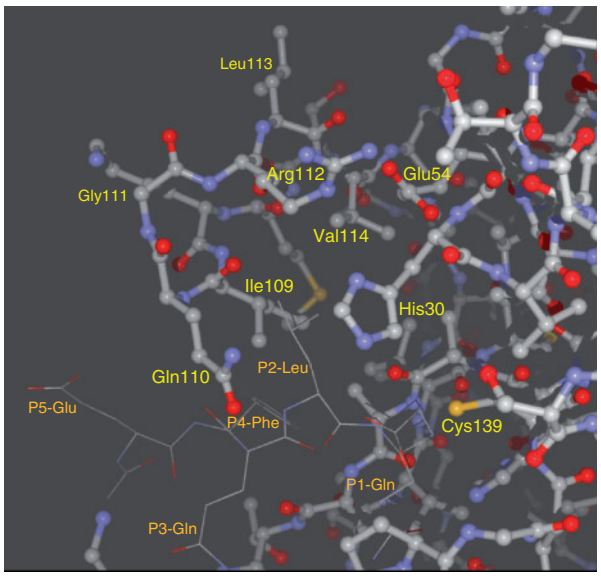

Fig. 5. **Structure model of the Chiba virus 3C-like protease with a peptide inhibitor.** Based on the X-ray structure of the inhibitor complex of the Southampton virus 3C-like protease (PDB ID: 2IPH), the structure of the Chiba virus protease was modelled as described in the experimental procedure. This depicts the vicinity of the active site of the protease. The residues in the protease are shown by balls and sticks, and the LGG peptide, a peptide inhibitor, is shown by a wire frame.

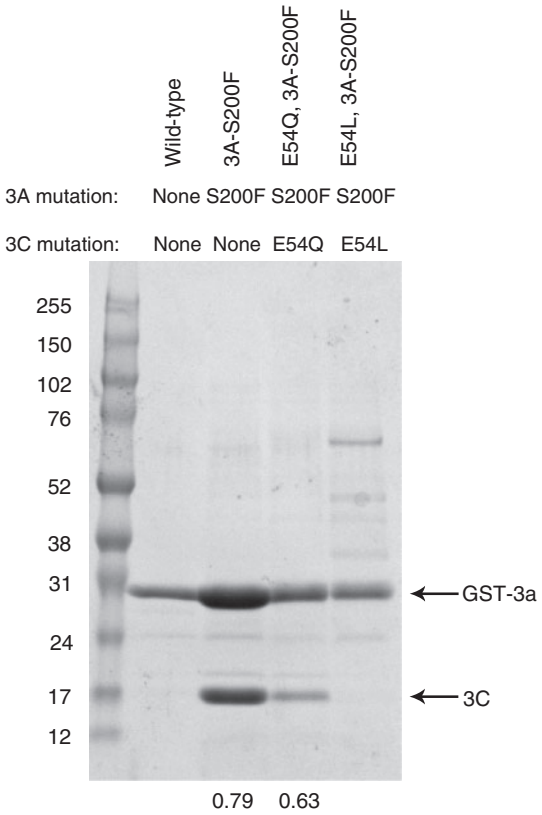

Fig. 6. **SDS–PAGE analysis of the proteins included in eluates from Glutathione Sepharose.** Cell extracts from the wild-type (containing neither 3A nor 3C mutations; Glu54, 3A-Ser200), 3A-S200F (Glu54, 3A-Phe200), E54Q, 3A-S200F (Gln54, 3A-Phe200) and E54L, 3A-S200F (Leu54, 3A-Phe200) fusion constructs were passed through Glutathione Sepharose. Proteins eluted by the addition of free glutathione were separated by SDS–PAGE. The numbers under the respective lanes indicate the density ratio of the 3C-like protease to GST-3a.

inhibitor complex of the Chiba virus protease based on the Southampton virus protease. Similar to the crystal structure of the Chiba virus protease (*13*), Glu54 is positioned at the bottom of the large S2 hydrophobic pocket, which consists of the hydrophobic parts of side chains of Ile109, Gln110 and Arg112, which are well conserved in various norovirus strains, and is apparently far away from both the P2 and P4 side chains. This suggested that the Leu mutation of Glu54 increases the hydrophobicity of the S2 pocket, and therefore the E54L protease requires a hydrophobic residue at the P2 position for effective proteolytic cleavage.

Effect of the Mutation of the 3A-Ser200 Residue on the Enzyme–Substrate Interaction—As described above, the cleavage pattern by the E54L protease was altered by the 3A-S200F mutation, and GST-3a was produced, indicating that the E54L protease cleaved the mutated (3A-S200F) 3A/3B junction (Figs 2 and 3). When the 3A-S200F mutation was introduced into the wild-type or E54Q mutant background, we found that the protease moiety was co-eluted with GST-3a in the GST-binding assay (Fig. 6). Especially, in the wild-type background, the density ratio of protease to GST-3a was significantly high compared to the E54Q background, as estimated by the density of respective protein bands. Since co-elution of the protease with GST-3a in the wild-type construct (3A-Ser200 and Glu54) did not happen (Fig. 6), the appearance of the protease in the 3A-S200F construct (Glu54 in the protease) was attributed solely to the 3A-S200F mutation. This result suggested that the protease was tightly bound to the C-terminus of the GST-3a protein.

To verify the complex formation of the protease and GST-3a, the eluates from Glutathione Sepharose of the wild-type and 3A-S200F extracts were separated by gel filtration. The first peak emerged earlier than that of the 44 kDa standard protein in both samples and the second peak was likely to correspond to the glutathione that the Glutathione Sepaharose eluates contained. Since the calculated molecular weight of GST-3a is 29.4 kDa, GST-3a proteins may be multimeric. SDS–PAGE analysis of the first peak clearly showed co-migration of the protease with GST-3a having the 3A-S200F mutation (Fig. 7). In addition, the ratio of the protease to GST-3a after gel filtration (0.77 in Fig. 7) was almost equal to that before chromatography (0.79 in Fig. 6). This result suggests that the protease may be tightly complexed with GST-3a, probably via the C-terminal 3A portion, and that the 3A-S200F mutation was solely responsible for this interaction.

To further understand the molecular aspect of the protease's interaction with the C-terminus of the 3A protein, various mutations were introduced at the Ser200 residue of 3A. As shown in Fig. 8A, despite the mutations

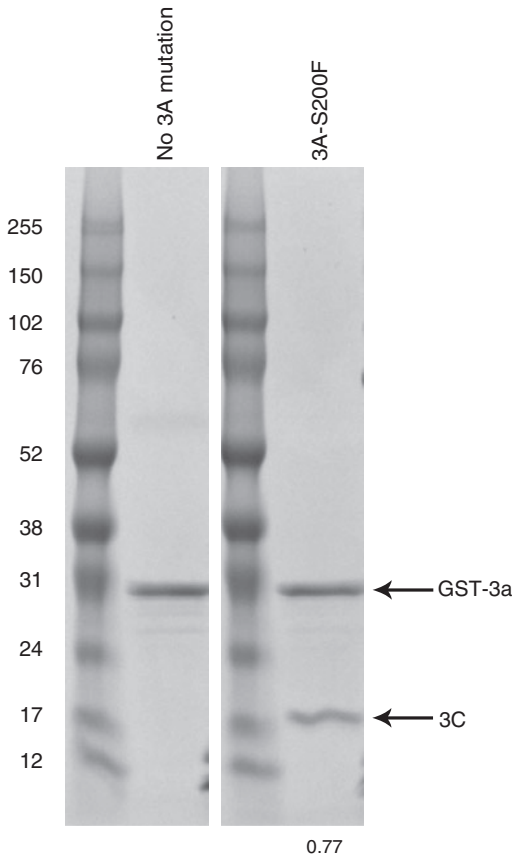

Fig. 7. **SDS–PAGE analysis of gel filtration chromatography isolates.** The final eluate from the wild-type ('No 3A mutation') or 3A-S200F construct obtained in Fig. 6 was subjected to gel filtration. The peak fractions of each chromatography were analysed by SDS–PAGE. The number under the gel indicates the density ratio of the 3C-like protease to GST-3a.

introduced at 3A-Ser200, the wild-type protease cleaved the 3A/3B junction, giving final products of GST-3a, 3B and 3C proteins. Coelution of the protease with GST-3a from Glutathione Sepharose was observed for the Leu, Met, Trp and Tyr mutants of the 3A-Ser200 residue besides the 3A-S200F mutant (Fig. 8B). However, this was not the case for the Ala and His mutants or for the wild-type (Ser). The GST-3a-to-protease ratios for the Phe, Leu and Trp mutants were slightly higher than those for the Met and Tyr mutants. The ratio for all samples was over 0.9 in SDS–PAGE gel of cell extract (Fig. 8A), suggesting that the high hydrophobicity of the side chain at position 200 of 3A was responsible for the interaction of the protease with the C-terminus of 3A.

Effect of the Mutation in the bII-cII Loop on the Enzyme–Substrate Interaction—The Ser200 residue of 3A corresponds to the P2 residue of the substrate. As described above, the P2 residue is surrounded by amino acid residues (Ile109, Gln110, Arg112 and Val114) in the loop region connecting two β-sheets, bII and cII (*13*). It is possible that the mutation in the bII-cII loop region affects the protease's interaction with the substrate. The Ala mutation was individually introduced to Ile109, Gln110, Arg112 or Val114, and their effect was examined in the presence or absence of the 3A-S200F mutation. None of the protease mutations apparently affected the cleavage at the 3A/3B and 3B/3C junctions, even if there was a S200F mutation in the C-terminus of 3A (Fig. 9A). As shown in Fig. 9B, when combined with the 3A-S200F mutation, all bII-cII loop mutations significantly reduced the amount of protease co-eluted with GST-3a. Especially, for the I109A mutation, no protease was co-eluted, indicating that the protease was rapidly released from the C-terminus of 3A after cleavage reaction. This suggested that the observed tight binding of the protease and GST-3a was attributable to the hydrophobicity of both the Ile109 residue of the protease and the Phe200 residue of the mutated 3A.

A smaller band (~27 kDa) than that of GST-3a was obvious in several eluates from Glutathione Sepharose, especially in the V114A mutant (Fig. 9B). This byproduct may arise from alternative processing at the site upstream from the 3A/3B junction by the mutant protease although the cleavage site was not identified in this study.

Effect of the Mutation of the 3A-Ala198 Residue on the Enzyme–Substrate Interaction—The E54L mutant protease required large hydrophobic residues at the P2 and P4 positions of the substrate for effective cleavage (Table 2), suggesting that the mutations of these two positions might affect each other, hence the enzyme–substrate interaction. The P4 residue at the 3A/3B junction is Ala198 of 3A. This residue was changed to Gly, Ser, or Val. The 3A-A198L mutation, mentioned in the first part of the results session, is also described here for comparison. The mutations themselves did not at all affect the cleavage by the wild-type protease (Fig. 10A). A combination of the A198S (Fig. 10B) or A198L (Fig. 10C) mutation with the S200F mutation completely eliminated the ability to co-elute with GST-3a, and the A198G and A198V mutations significantly reduced the amount of co-eluted protease (Fig. 10B). It was likely that the tight binding of the protease with the C-terminus caused by the 3A-S200F mutation at the P2 position was sensitive to the mutation of the P4 residue. The Ala residue was the most favourable for tight binding, but the increase in hydrophobicity (Val and Leu) or the presence of a hydrophilic residue (Ser) resulted in a rapid release of the product from the binding site in the protease.

DISCUSSION

The Glu54 residue is implicated as the third-member carboxylate of the catalytic triad (Glu54-His30-Cys139) (*12*, *13*, *18*). In a previous paper (*14*), we found that the GST-3aBC fusion protein, including the E54I, E54L, or E54P mutant 3C-like protease, underwent cleavage at the 3B/3C junction, but not at the 3A/3B junction, which resulted in the accumulation of the GST-3aB intermediate as well as the release of the mutant protease. This result raised two possibilities: (i) the E54I, E54L or E54P mutant protease is inactivated immediately when it is released after the cleavage event at the 3B/3C junction, and (ii) the mutant

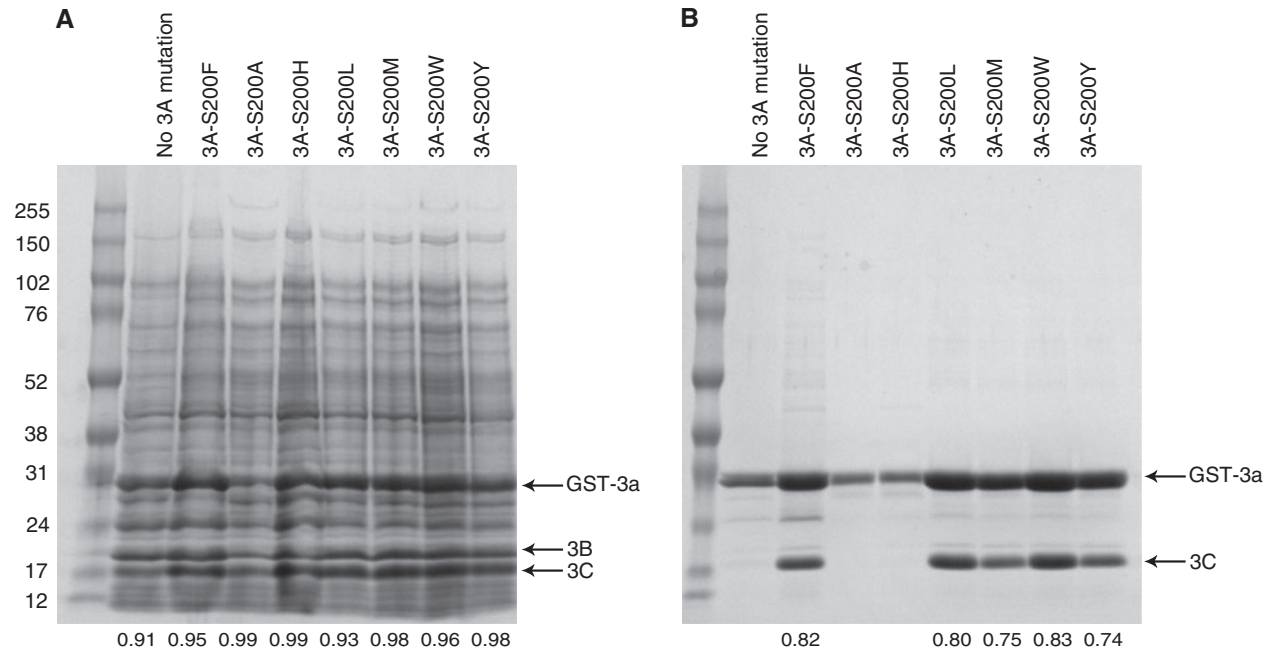

Fig. 8. **Effect of the 3A-Ser200 mutation on the enzyme (wild-type protease)–substrate interaction.** SDS–PAGE analysis was done as described in Fig. 2. (A) SDS–PAGE of cell extracts including 15 μg of proteins. (B) SDS–PAGE of the eluates obtained in the GST-binding assay. The numbers under the respective lanes indicate the density ratio of the 3C-like protease to GST-3a.

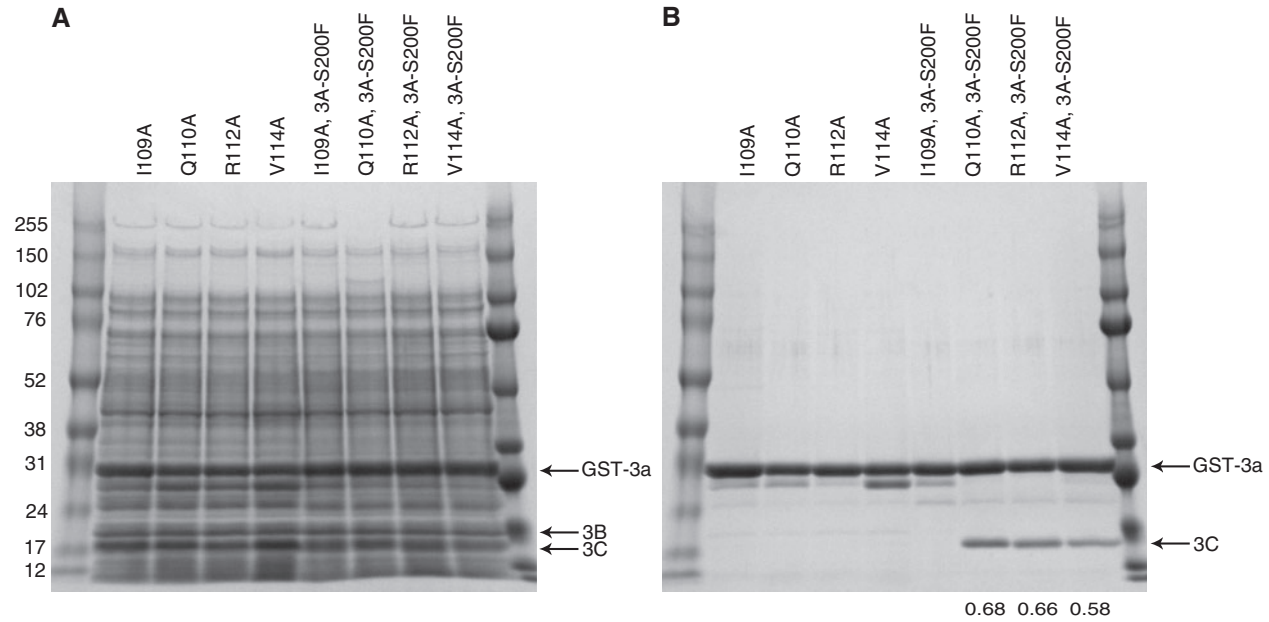

Fig. 9. **Effect of the bII-cII loop mutation on the enzyme–substrate interaction.** SDS–PAGE analysis was done as described in Fig. 2. (A) SDS–PAGE of cell extracts including 15 μg of proteins. (B) SDS–PAGE of the eluates obtained in the GST-binding assay. The numbers under the respective lanes indicate the density ratio of the 3C-like protease to GST-3a.

proteases favour the 3B/3C sequence over the 3A/3B sequence. In this report, we investigated the latter possibility by generating various junction mutants, based on the GST-3aBC fusion protein including the wild-type, E54Q or E54L 3C-like protease. These results reinforced the different properties of the E54L mutant protease and clearly showed that the E54L protease required the large hydrophobic amino acid residues at the P4 and P2 positions in order to cleave the substrate. This indicated that the 3C-like protease sensed the chemical nature of the

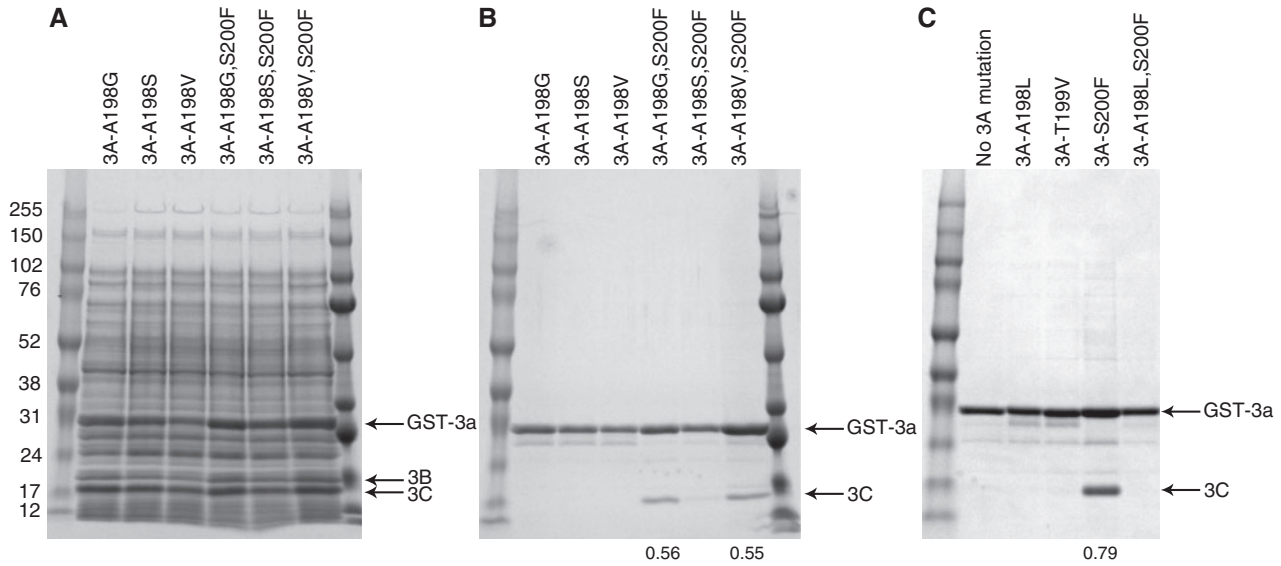

Fig. 10. **Effect of the 3A-Ala198 mutation on the enzyme (wild-type protease)–substrate interaction.** SDS–PAGE analysis was done as described in Fig. 2. (A) SDS–PAGE of cell extracts including 15 μg of proteins. (B, C) SDS–PAGE of the eluates obtained in the GST-binding assay. The numbers under the respective lanes indicate the density ratio of the 3C-like protease to GST-3a.

side chain at the P4 and P2 positions, although the wild-type protease recognized and cleaved the 3A/3B and 3C/3D junctions at which any of the mutations was introduced. It was concluded that the E54L mutant protease had a narrower substrate spectrum than the wild-type protease. Therefore, Glu54 is not involved directly in mediating proteolytic activity, but it affects the substrate specificity.

As shown in Figs 2 and 3 the E54L mutant protease effectively cleaved both the 3A/3B and 3B/3C junctions of the ATStoLSF mutant and 3A-A198L,S200F double mutant, which had the Leu and Phe residues at the P4 and P2 positions, respectively. However, in the ABtoBC mutant fusion protein, almost no cleavage occurred at the mutated 3A/3B junction although it had the Leu and Phe residues at the P4 and P2 positions, respectively. The only difference was the two residues at the N-terminus of the 3B protein. That is, the N-terminus of the ATStoLSF mutant and that of 3A-A198L, S200F double mutant begin with Gly-Lys, which is the same as in the case of the wild-type fusion protein, whereas that of the ABtoBC mutant begins with Ala-Pro. This might be caused by the difference between the conformation of the 3A/3B junction and that of the 3B/3C junction, although there is no structural evidence to support this.

The 3A-A198L, S200F double mutant has the Leu198-Thr-Phe sequence and the Leu133-Ser-Phe sequence at the 3A/3B and 3B/3C junctions, respectively. The E54L mutant protease cleaved both sequences described above. On the other hand, in the 3A-S200F single mutant, although there was the Leu133-Ser-Phe sequence at the 3B/3C junction, the E54L mutant protease seemed to initially attack the Ala198-Thr-Phe sequence at the 3A/3B junction, since the band corresponding to the 3BC intermediate as well as the GST-3a was observed with trace amounts of 3B and 3C. This result was inconsistent with the fact that the fusion protein including only the E54L mutation in the protease moiety gave the GST-3aB intermediate and 3C (*14*) (Fig. 2). It was surprising that the single amino acid change in the cleavage site altered the preference of the protease. It seemed that the Ala-Thr-Phe sequence was less hydrophobic than the Leu-Ser-Phe and Leu-Thr-Phe sequences. Therefore, the conformation of the peptide around the cleavage site might also be important for recognition by the protease.

Recently, the crystal structure of the 3C-like protease from the Southampton strain (*16*, *17*) was resolved as a complex with a peptide inhibitor (PDB ID: 2IPH). Although we had resolved the structure of the 3C-like protease from the Chiba strain (*13*), the complex of the Chiba virus protease with an inhibitor was modelled based on the structure of the Southampton virus protease. These two proteases share 90% identity on the amino acid level, the similarity score being almost 100%. All the residues depicted in Fig. 5 are conserved in the two proteases. Overall structures of these proteases are similar, except that the bII-cII loop in the inhibitor complex is bent so as to cover the S2 hydrophobic pocket that accommodated the P2 side chain of the substrate. This is probably because of the presence of an inhibitor, the LGG peptide. As shown in Fig. 5 and also in our previous paper (*13*), the Glu54 residue was located at the bottom of the S2 hydrophobic pocket. Modelling was sufficient to let us estimate that the E54L mutation intensified the hydrophobicity of the S2 pocket, consistent with the results that the E54L protease required hydrophobic amino acid residues at the P2 position of the substrate for an efficient cleavage. On the other hand, the P4 side chain was also surrounded by the hydrophobic components, but was far from the Glu54 residue. In the modelling, it was not obvious whether

the E54L mutation affected the property of the S4 hydrophobic pocket or not (data not shown). The E54L protease might have the altered S4 pocket, but a structural analysis is necessary. It should be noted that the third-member carboxylate of the catalytic triad affects the substrate specificity. This phenomenon raises new insight into the mechanism of the catalysis by all the proteases belonging to the chymotrypsin-like protease family.

In the series of mutational analysis, we found that the wild-type protease was tightly bound to the C-terminus of GST-3a including the S200F mutation of the 3A protein (Figs 6 and 7). Since the wild-type protease was never co-eluted with GST-3a possessing the original 3A sequence, this interaction was attributed solely to the Phe mutation of the 3A-Ser200 residue, P2 position of the substrate. The presence of a large hydrophobic amino acid (Phe, Leu, Met, Trp or Tyr) at this position retained tight binding, but a small (Ala) or hydrophilic (His) residue resulted in a loss of binding (Fig. 8). It was interesting that the interaction was sensitive to the mutation of the residues in the bII-cII loop region, which was in close proximity to the active site of the protease (Fig. 9), or to the mutation of the P4 residue of the substrate (Fig. 10). It was also notable that the protease was not bound to the C-terminus of the cleaved 3B protein containing the KLSFE sequence whose P2 position was occupied by the Phe residue. Tight binding was not observed for the 3A-A198L, S200F (Fig. 10C) and the ATStoLSF (with the wild-type protease) mutants (data not shown). These results suggest that the kinetics of the protease correlate with the chemical nature of amino acid residues at the P2 and P4 positions of the substrate. The increase in the hydrophobicity of the P2 residue in the 3A/3B junction intensified the degree of the interaction between the protease and the C-terminus of 3A (Fig. 8). This reflects the lowered release rate of the final product from the enzyme, since it was clear that the protease completed the proteolytic reaction as shown in the appearance of two bands corresponding to GST-3a and the protease (Figs 6–8). It was therefore concluded that the amino acid residue at position 200 of 3A was involved in the release step from the active site of the protease. It would be disadvantageous in nature that the mutation inhibited the release of the product from the enzyme, and therefore such mutations at the cleavage sites would never occur. On the contrary, this kind of mutations may be helpfully used to design inhibitors of the norovirus 3C-like proteases and related proteases.

The bII-cII loop of the norovirus 3C-like protease geometrically corresponds to the β-ribbon described in the 3C proteases from picornaviruses such as poliovirus (*19*) and foot-and-mouth disease virus (FMDV) (*20*). In the FMDV 3C protease, it was shown that the β-ribbon of interest was involved in substrate recognition as well as catalytic activity (*20*). In an analogous finding, the mutation in the bII-cII loop of the norovirus protease clearly affected the enzyme–substrate interaction (Fig. 9). It is likely that the hydrophobic residue at position 109 (Ile109) of the protease is involved in recognition of the P2 residue of the substrate since the I109A mutation led to a rapid release of the final product (GST-3a with 3A-S200F) from the protease (Fig. 9).

The P4 residue at the 3A/3B junction is the Ala198 residue of the 3A protein. The amino acid change at this position dramatically altered the degree of enzyme–substrate interaction based on the 3A-S200F mutation (Fig. 10). The increases in both hydrophilicity (Ser and Gly) and hydrophobicity (Val and Leu) diminished or eliminated the interaction. According to the crystal structures (*13*, *18*) (see also PDB ID: 2IPH), the Ile109 residue in the bII-cII loop is involved in the recognition of both P2 and P4 side chains. This suggested that P2 and P4 side chains sense each other via the Ile109 side chain in the protease during the proteolytic reaction. It should be noted that the bII-cII loop is highly flexible; especially, the structure of this loop bends to hold an inhibitor in the Southampton virus protease, compared to the corresponding region of the Chiba virus (*13*) or Norwalk virus (*18*) counterparts. This suggests that the bII-cII loop moves in and out in association with the entry of the substrate into and the release of the product from the active site. It is concluded that the bII-cII loop in the norovirus 3C-like protease and the β-ribbon, the corresponding loop region found in picornavirus 3C proteases (*19–21*) and related chymotrypsin-like serine proteases (*22*, *23*), plays a universal role in substrate recognition.

FUNDING

Grant-in-aid from the Ministry of Health, Labour and Welfare, Japan.

CONFLICT OF INTEREST

None declared.

REFERENCES

1. Estes, M.K., Prasad, B.V., and Atmar, R.L. (2006) Noroviruses everywhere: has something changed? *Curr. Opin. Infect. Dis.* **19**, 467–474
2. Goodgame, R. (2007) Norovirus gastroenteritis. *Curr. Infect. Dis. Rep.* **8**, 401–408
3. Hansman, G. S., Natori, K., Shirato-Horikoshi, H., Ogawa, S., Oka, T., Katayama, K., Tanaka, T., Miyoshi, T., Sakae, K., Kobayashi, S., Shinohara, M., Uchida, K., Sakurai, N., Shinozaki, K., Okada, M., Seto, Y., Kamata, K., Nagata, N., Tanaka, K., Miyamura, T., and Takeda, N. (2006) Genetic and antigenic diversity among noroviruses. *J. Gen. Virol.* **87**, 909–919
4. Daughenbaugh, K.F., Fraser, C.S., Hershey, J.W., and Hardy, M.E. (2003) The genome-linked protein VPg of the Norwalk virus binds eIF3, suggesting its role in translation initiation complex recruitment. *EMBO J.* **22**, 2852–2859
5. Liu, B., Clarke, I. N., Caul, E.O., and Lambden, P.R. (1995) Human enteric caliciviruses have a unique genome structure and are distinct from the Norwalk-like viruses. *Arch. Virol.* **140**, 1345–1356
6. Belliot, G., Sosnovtsev, S.V., Mitra, T., Hammer, C., Garfield, M., and Green, K.Y. (2003) In vitro proteolytic processing of the MD145 norovirus ORF1 nonstructural polyprotein yields stable precursors and products similar to those detected in calicivirus-infected cells. *J. Virol.* **77**, 10957–10974
7. Sosnovtsev, S.V., Belliot, G., Chang, K.O., Prikhodko, V.G., Thackray, L.B., Wobus, C.E., Karst, S.M., Virgin, H.W., and Green, K.Y. (2006) Cleavage map and proteolytic processing

of the murine norovirus nonstructural polyprotein in infected cells. *J. Virol.* **80**, 7816–7831
8. Prasad, B.V., Hardy, M.E., Dokland, T., Bella, J., Rossmann, M.G., and Estes, M.K. (1999) X-ray crystallographic structure of the Norwalk virus capsid. *Science* **286**, 287–290
9. Cao, S., Lou, Z., Tan, M., Chen, Y., Liu, Y., Zhang, Z., Zhang, X.C., Jiang, X., Li, X., and Rao, Z. (2007) Structural basis for the recognition of blood group trisaccharides by norovirus. *J. Virol.* **81**, 5949–5957
10. Lochridge, V.P. and Hardy, M.E. (2007) A single-amino-acid substitution in the P2 domain of VP1 of murine norovirus is sufficient for escape from antibody neutralization. *J. Virol.* **81**, 12316–12322
11. Shirato-Horikoshi, H., Ogawa, S., Wakita, T., Takeda, N., and Hansman, G.S. (2007) Binding activity of norovirus and sapovirus to histo-blood group antigens. *Arch. Virol.* **152**, 457–461
12. Someya, Y., Takeda, N., and Miyamura, T. (2002) Identification of active-site amino acid residues in the Chiba virus 3C-like protease. *J. Virol.* **76**, 5949–5958
13. Nakamura, K., Someya, Y., Kumasaka, T., Ueno, G., Yamamoto, M., Sato, T., Takeda, N., Miyamura, T., and Tanaka, N. (2005) A norovirus protease structure provides insights into active and substrate binding site integrity. *J. Virol.* **79**, 13685–13693
14. Someya, Y., Takeda, N., and Wakita, T. (2008) Saturation mutagenesis reveals that Glu54 of norovirus 3C-like protease is not essential for the proteolytic activity. *J. Biochem.* **144**, 771–780
15. Someya, Y., Takeda, N., and Miyamura, T. (2000) Complete nucleotide sequence of the Chiba virus genome and functional expression of the 3C-like protease in Escherichia coli. *Virology* **278**, 490–500
16. Lambden, P.R., Caul, E.O., Ashley, C.R., and Clarke, I.N. (1993) Sequence and genome organization of a human small round-structured (Norwalk-like) virus. *Science* **259**, 516–519
17. Liu, B., Clarke, I.N., and Lambden, P.R. (1996) Polyprotein processing in Southampton virus: identification of 3C-like protease cleavage sites by in vitro mutagenesis. *J. Virol.* **70**, 2605–2610
18. Zeitler, C.E., Estes, M.K., and Prasad, B.V.V. (2006) X-ray crystallographic structure of the Norwalk virus protease at 1.5-Å resolution. *J. Virol.* **80**, 5050–5058
19. Mosimann, S.C., Cherney, M.M., Sia, S., Plotch, S., and James, M.N.G. (1997) Refined X-ray crystallographic structure of the poliovirus 3C gene product. *J. Mol. Biol.* **273**, 1032–1047
20. Sweeney, T.R., Roqué-Rosell, N., Birtley, J.R., Leatherbarrow, R.J., and Curry, S. (2007) Structural and mutagenic analysis of foot-and-mouth disease virus 2C proteae reveals the role of the β-ribbon in proteolysis. *J. Virol.* **81**, 115–124
21. Matthews, D.A., Dragovich, P.S., Webber, S.E., Fuhrman, S.A., Patick, A.K., Zalman, L.S., Hendrickson, T.F., Love, R.A., Prins, T.J., Marakovits, J.T., Zhou, R., Tikhe, J., Ford, C.E., Meador, J.W., Ferre, R.A., Brown, E.L., Binford, S.L., Brothers, M.A., DeLisle, D. M., and Worland, S.T. (1999) Structure-assisted design of mechanism-based irreversible inhibitors of human rhinovirus 3C protease with potent antiviral activity against multiple rhinovirus serotypes. *Proc. Natl Acad. Sci. USA* **96**, 11000–11007
22. James, M.N.G., Sielecki, A.R., Brayer, G.D., Delbaere, L.T.J., and Bauer, C.-A. (1980) Structures of product and inhibitor complexes of Streptomyces griseusprotease A at 1.8 Å resolution: a model for serine protease catalysis. *J. Mol. Biol.* **144**, 43–88
23. Fujinaga, M., Delbaere, L.T.J., Brayer, G.D., and James, M.N.G. (1985) Refined structure of α-lytic protease at 1.7 Å resolution analysis of hydrogen bonding and solvent structure. *J. Mol. Biol.* **184**, 479–502